

OPAQUE MINERALS IN ANTARCTIC CO<sub>3</sub> CARBONACEOUS  
CHONDRITES, YAMATO-74135, -790992, -791717, -81020, -81025, -82050  
AND ALLAN HILLS-77307

Yasuhiro SHIBATA

*Department of Earth and Planetary Sciences, Faculty of Science, Hokkaido University,  
Kita-10, Nishi-8, Kita-ku, Sapporo 060*

**Abstract:** Metamorphic sequence and mineralogy of opaque minerals of Antarctic seven CO<sub>3</sub> chondrites, Yamato (Y)-74135, Y-790992, Y-791717, Y-81020, Y-81025, Y-82050 and Allan Hills (ALH)-77307 was studied by an optical, scanning electron microscope and electron microprobe technique. Based on olivine and chromite compositions, Y-74135, Y-81020 and Y-81025 are classified as least metamorphosed CO<sub>3</sub> chondrites. Metamorphic grades of these three chondrites are the same as or less than that of ALH-77307. Whereas metamorphic grades of Y-790992, Y-791717 and Y-82050 are higher than that of ALH-77307.

The three least metamorphosed chondrites include cohenite abundantly. Judging from the mode of occurrence of cohenite, cohenite would have formed not by the diffusion of carbon into solid Fe-Ni metal, but by crystallization from Fe-Ni-C melt. Fine-grained tetrataenite within kamacite suggest that precipitation of the tetrataenite occurred under the condition in which Ni movement in kamacite was sluggish extremely (probably below 450°C). In Y-81025, assemblage of spherical magnetite like as framboidal magnetite in CI chondrites was observed. It would be also one of evidences of the low-temperature condition which the least metamorphosed chondrites in this study were situated. In Y-81025 and Y-74135, there are fine-grained perryite and phosphide.

Although previous workers have already pointed out that primitive chondrites often have carbides, this study make clear that the existence of cohenite is indeed one of the essential properties in least metamorphosed CO<sub>3</sub> chondrites.

## 1. Introduction

Previous workers have studied a metamorphic sequence of CO<sub>3</sub> chondrites from the viewpoint of silicate composition, thermoluminescence (TL) sensitivity, alteration of CAIs (*e.g.*, McSWEEN, 1977; SCOTT and JONES, 1990; SEARS *et al.*, 1991; KOJIMA *et al.*, 1995). However, there is not much the study of opaque minerals in low-metamorphic grade CO<sub>3</sub> chondrites. A few studies attended to opaque minerals in low metamorphosed CO<sub>3</sub> chondrites; for example, cohenite in ALHA77307 (SCOTT and JONES, 1990), no carbide in Colony meteorite (RUBIN *et al.*, 1985) and a brief comment on opaque minerals in primitive chondrites (SEARS *et al.*, 1991).

It is very important to specify the nature of opaque minerals in low-metamorphic grade CO<sub>3</sub> chondrites for discussion about textural and compositional changes of opaque minerals through a metamorphic sequence.

In this study metamorphic grades of eight CO3 chondrites based on petrographical investigations were determined and the detailed description of opaque minerals, especially cohenite, in low-metamorphic grade CO3 chondrites was carried out.

## 2. Materials and Methods

Polished thin sections of Y-74135, Y-790992, Y-791717, Y-81020, Y-81025, Y-82050 and ALH-77307 supplied by National Institute of Polar Research (NIPR) were used in this study. Chemical analyses were made by a wavelength dispersive electron microprobe analyzer (EPMA, JEOL Superprobe-733). EPMA analyses were carried out at an accelerating voltage of 15 kV and the beam current of 20 to 40 nA. Cobalt background counts were taken at wavelengths of about 177.4 and 180.8 pm in order to eliminate the contribution of FeK $\alpha$  radiation to the CoK $\alpha$  peak. ZAF corrections were applied for measured X-ray relative intensity (YUI, 1992). Qualitative analyses of carbon were made by the analyzing crystal (lead stearate) on EPMA spectrometer.

## 3. Results

### 3.1. Chemistry of olivine and chromite

Samples studied here are composed of several constituents common CO3 chondrites; chondrules, mineral fragments, opaque mineral clots and matrices. Most chondrules are porphyritic chondrules (porphyritic olivines, porphyritic olivine-pyroxenes and porphyritic pyroxenes), and some chondrules closely resemble type IA or type II chondrule defined by SCOTT and TAYLOR (1983). The opaque mineral clots are mainly composed of Fe-Ni metal and/or sulfide minerals (troilite and/or pyrrhotite). However, there are different from details of the opaque mineral assemblages among samples. Therefore, the detail description for opaque minerals shows in later sections.

Table 1 shows the result of analyses of randomly selected olivine and low-Ca pyroxene grains in samples studied here. Mean fayalite content (Fa mol%) is 5.3 in Y-81020, 5.2 in Y-81025, 7.4 in Y-74135, 12.5 in ALH-77307, 12.7 in Y-82050, 15.6 in Y-790992 and 16.8 in Y-791717. Y-81020 and Y-81025 was regarded as paired samples in previous work (YANAI and KOJIMA, 1987). In this study, Y-81020 and Y-81025 closely

Table 1. Average compositions of randomly selected olivines and low-Ca pyroxenes in seven CO3 chondrites.

| Meteorite | Olivine   |          |           |          |                 | Low-Ca pyroxene |          |                 |
|-----------|-----------|----------|-----------|----------|-----------------|-----------------|----------|-----------------|
|           | Fa (mol%) |          | CaO (wt%) |          | No. of crystals | Fs (mol%)       |          | No. of crystals |
|           | Mean      | $\sigma$ | Mean      | $\sigma$ |                 | Mean            | $\sigma$ |                 |
| Y-81020   | 5.3       | 11       | 0.27      | 0.13     | 40              | 2.3             | 5.3      | 25              |
| Y-81025   | 5.2       | 11       | 0.27      | 0.13     | 47              | 2.9             | 4.2      | 38              |
| Y-74135   | 7.4       | 13       | 0.28      | 0.17     | 46              | 2.4             | 2.2      | 26              |
| ALH-77307 | 12.5      | 17       | 0.23      | 0.09     | 46              | 3.7             | 7.6      | 26              |
| Y-82050   | 12.7      | 14       | 0.24      | 0.14     | 57              | 2.9             | 3.2      | 16              |
| Y-790992  | 15.6      | 15       | 0.22      | 0.12     | 66              | 2.9             | 3.6      | 19              |
| Y-791717  | 16.8      | 15       | 0.24      | 0.14     | 70              | 1.9             | 1.8      | 20              |

resembles in mean fayalite and CaO content (Table 1). These samples is considered as the same rock in the following.

Figure 1 shows the representative zoning profiles for minor elements taken from core to rim of the olivine grain in type IA chondrule in ALH-77307, Y-81025, Y-74135 and Y-791717. Olivines in type IA chondrule in ALH-77307, Y-81025 and Y-74135 are poorer in Fe and richer in Cr toward rims, whereas that in Y-791717 is richer in Fe, and show strong Fe-Mg zoning, poorer in Cr and show flat Cr zoning.

Chromites in type II chondrule occur at the margins of olivines. Chromites are euhedral or subhedral shape, and typically <20  $\mu\text{m}$  in size. Figure 2 shows the representative occurrence of olivine and coexisting chromite in type II chondrule. Table 2 shows the chemical compositions of coexisting olivine and chromite in type II chondrule in samples studied here. Analyzed points for olivine and chromite are near the grain boundary of both phases. Figure 3 shows Fe-Mg partitioning between olivine edges and chromite in type II chondrules ( $K_D = (\text{Fe}/\text{Mg})^{\text{spinel}} / (\text{Fe}/\text{Mg})^{\text{olivine}}$ ) against the Cr/(Cr+Al) ratio in chromites. Isotherms and the data of ALH-77307 (filled circles) are quoted from JOHNSON

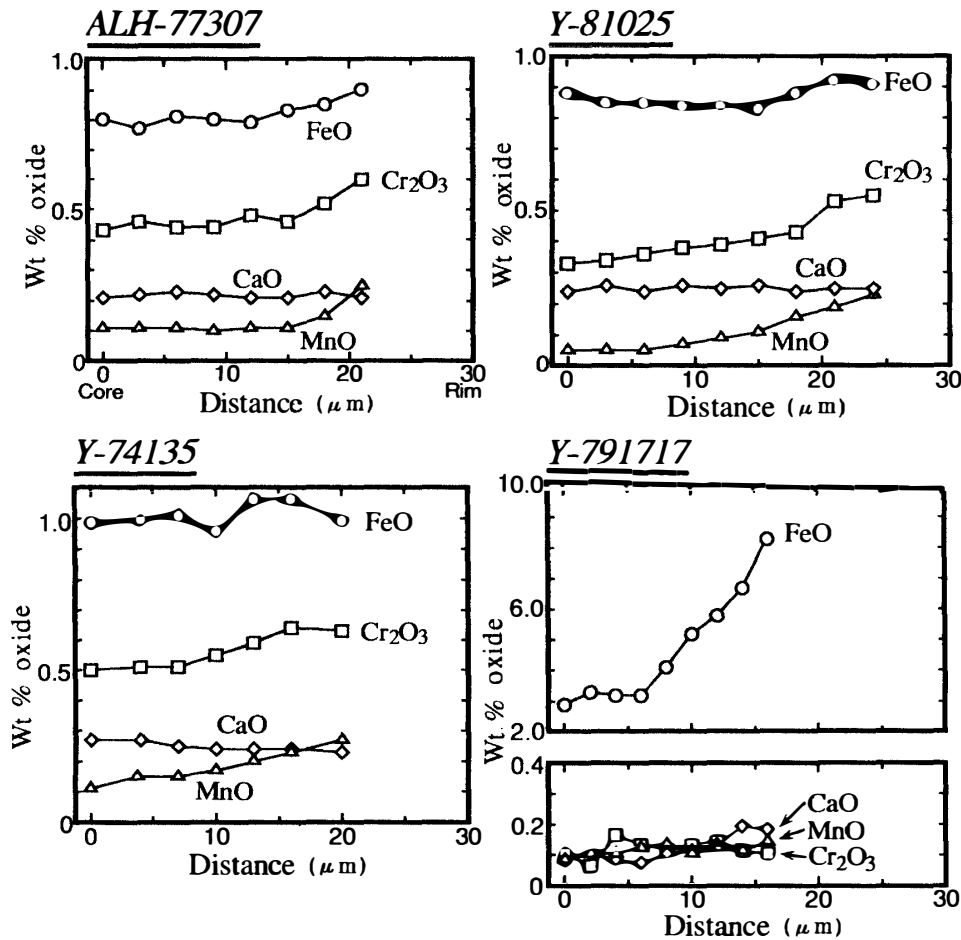


Fig. 1. Representative zoning profiles for FeO, Cr<sub>2</sub>O<sub>3</sub>, CaO and MnO taken from core to rim of olivine grain in type IA chondrules in ALH-77307, Y-81025, Y-74135 and Y-791717.

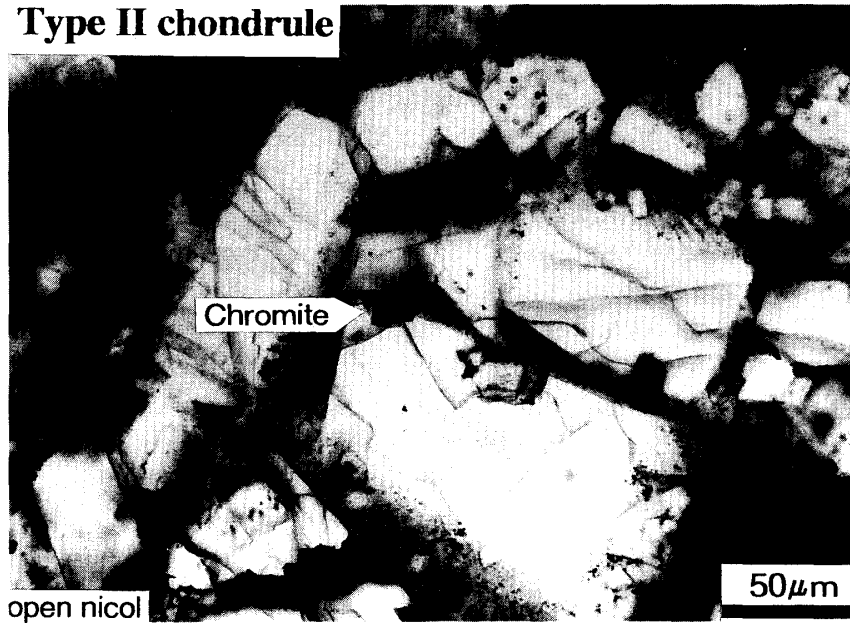


Fig. 2. The mode of occurrence of olivine and coexisting chromite in type II chondrule in Y-791717.

Table 2. Chemical compositions (wt%) of coexisting olivine (ol) and chromite (sp) in type II chondrule. Analyzed points for olivine and chromite are near the grain boundary of both phases.

| Meteorite | Chondrule<br>(ol/sp) | SiO <sub>2</sub> | TiO <sub>2</sub> | Al <sub>2</sub> O <sub>3</sub> | FeO   | MgO   | Cr <sub>2</sub> O <sub>3</sub> | MnO  | V <sub>2</sub> O <sub>3</sub> | CaO  | Total  |
|-----------|----------------------|------------------|------------------|--------------------------------|-------|-------|--------------------------------|------|-------------------------------|------|--------|
| Y-81020   | PO4 (sp)             | 0.34             | 0.77             | 17.83                          | 24.64 | 7.54  | 47.21                          | 0.16 | 0.57                          | 0.03 | 99.09  |
|           | (ol)                 | 36.46            | 0.01             | 0.05                           | 30.05 | 31.04 | 0.42                           | 0.38 | 0.00                          | 0.51 | 98.92  |
| Y-81025   | PO1 (sp)             | 0.20             | 0.59             | 15.99                          | 24.15 | 8.48  | 51.48                          | 0.19 | 0.48                          | 0.06 | 101.62 |
|           | (ol)                 | 38.22            | 0.00             | 0.07                           | 24.43 | 37.48 | 0.65                           | 0.30 | 0.00                          | 0.28 | 101.43 |
|           | PO4 (sp)             | 0.22             | 1.29             | 13.98                          | 26.55 | 5.95  | 51.07                          | 0.27 | 0.72                          | 0.09 | 100.14 |
|           | (ol)                 | 37.13            | 0.02             | 0.01                           | 30.22 | 32.41 | 0.34                           | 0.48 | 0.00                          | 0.29 | 100.90 |
|           | PO9 (sp)             | 0.25             | 0.93             | 15.14                          | 26.66 | 6.93  | 49.86                          | 0.25 | 0.69                          | 0.09 | 100.80 |
|           | (ol)                 | 37.73            | 0.01             | 0.05                           | 26.07 | 36.14 | 0.65                           | 0.32 | 0.03                          | 0.25 | 101.25 |
| Y-74135   | PO13 (sp)            | 0.22             | 0.51             | 15.78                          | 25.44 | 7.18  | 50.68                          | 0.19 | 0.52                          | 0.02 | 100.54 |
|           | (ol)                 | 37.76            | 0.00             | 0.05                           | 27.50 | 34.34 | 0.69                           | 0.34 | 0.02                          | 0.24 | 100.94 |
|           | PO14 (sp)            | 0.25             | 0.71             | 16.89                          | 23.38 | 8.50  | 50.32                          | 0.18 | 0.67                          | 0.05 | 100.95 |
|           | (ol)                 | 38.27            | 0.00             | 0.06                           | 25.20 | 36.18 | 0.76                           | 0.34 | 0.00                          | 0.31 | 101.12 |
|           | PO15 (sp)            | 0.36             | 0.88             | 15.42                          | 26.19 | 7.07  | 50.68                          | 0.24 | 0.55                          | 0.04 | 101.43 |
|           | (ol)                 | 36.71            | 0.03             | 0.04                           | 32.58 | 30.15 | 0.67                           | 0.41 | 0.00                          | 0.34 | 100.93 |
|           | PO16 (sp)            | 0.26             | 0.46             | 17.92                          | 24.67 | 8.36  | 48.26                          | 0.17 | 0.44                          | 0.01 | 100.55 |
|           | (ol)                 | 38.06            | 0.02             | 0.04                           | 27.22 | 34.76 | 0.38                           | 0.28 | 0.00                          | 0.34 | 101.10 |
| ALH-77307 | PO5 (sp)             | 0.29             | 0.93             | 21.44                          | 26.33 | 6.52  | 43.41                          | 0.24 | 0.75                          | 0.09 | 100.00 |
|           | (ol)                 | 37.32            | 0.00             | 0.07                           | 31.54 | 30.40 | 0.71                           | 0.43 | 0.03                          | 0.28 | 100.78 |
| Y-82050   | PO1 (sp)             | 0.27             | 1.18             | 13.70                          | 32.06 | 1.84  | 49.90                          | 0.20 | 0.65                          | 0.07 | 99.87  |
|           | (ol)                 | 37.22            | 0.01             | 0.01                           | 31.26 | 31.67 | 0.24                           | 0.26 | 0.01                          | 0.23 | 100.91 |

Table 2. (Continued)

| Meteorite | Chondrule (ol/sp) | SiO <sub>2</sub> | TiO <sub>2</sub> | Al <sub>2</sub> O <sub>3</sub> | FeO   | MgO   | Cr <sub>2</sub> O <sub>3</sub> | MnO  | V <sub>2</sub> O <sub>3</sub> | CaO  | Total  |
|-----------|-------------------|------------------|------------------|--------------------------------|-------|-------|--------------------------------|------|-------------------------------|------|--------|
| Y-82050   | PO2 (sp)          | 0.21             | 0.61             | 12.23                          | 32.18 | 1.80  | 51.39                          | 0.22 | 0.53                          | 0.12 | 99.29  |
|           | (ol)              | 36.27            | 0.00             | 0.04                           | 35.02 | 28.36 | 0.17                           | 0.35 | 0.01                          | 0.32 | 100.54 |
|           | PO3 (sp)          | 0.28             | 1.16             | 7.49                           | 32.47 | 1.28  | 57.35                          | 0.22 | 0.67                          | 0.11 | 101.03 |
|           | (ol)              | 36.01            | 0.01             | 0.01                           | 38.47 | 26.01 | 0.50                           | 0.33 | 0.00                          | 0.20 | 101.54 |
|           | PO10 (sp)         | 0.26             | 1.36             | 10.00                          | 32.70 | 1.24  | 52.81                          | 0.23 | 0.95                          | 0.14 | 99.69  |
|           | (ol)              | 35.50            | 0.00             | 0.02                           | 39.38 | 24.53 | 0.25                           | 0.42 | 0.02                          | 0.26 | 100.38 |
| Y-790992  | PO2 (sp)          | 0.20             | 0.49             | 15.13                          | 30.39 | 3.31  | 50.38                          | 0.18 | 0.38                          | 0.08 | 100.54 |
|           | (ol)              | 36.80            | 0.01             | 0.04                           | 33.15 | 30.33 | 0.21                           | 0.30 | 0.00                          | 0.14 | 100.98 |
|           | PO3 (sp)          | 0.24             | 0.69             | 16.12                          | 31.56 | 2.79  | 47.80                          | 0.21 | 0.41                          | 0.11 | 99.93  |
|           | (ol)              | 35.96            | 0.02             | 0.01                           | 35.86 | 27.85 | 0.18                           | 0.36 | 0.00                          | 0.26 | 100.50 |
|           | PO5 (sp)          | 0.30             | 1.44             | 13.76                          | 32.88 | 2.06  | 48.19                          | 0.24 | 0.62                          | 0.06 | 99.55  |
|           | (ol)              | 36.34            | 0.00             | 0.03                           | 33.63 | 29.16 | 0.25                           | 0.28 | 0.00                          | 0.17 | 99.86  |
|           | PO7 (sp)          | 0.28             | 0.68             | 14.45                          | 31.99 | 2.03  | 48.32                          | 0.14 | 0.56                          | 0.05 | 98.50  |
|           | (ol)              | 37.57            | 0.01             | 0.05                           | 29.90 | 32.98 | 0.14                           | 0.30 | 0.00                          | 0.15 | 101.10 |
| Y-791717  | PO1 (sp)          | 0.31             | 0.70             | 3.99                           | 31.48 | 1.29  | 60.41                          | 0.23 | 0.57                          | 0.12 | 99.10  |
|           | (ol)              | 35.96            | 0.01             | 0.05                           | 37.44 | 26.13 | 0.42                           | 0.40 | 0.00                          | 0.20 | 100.61 |
|           | PO2 (sp)          | 0.37             | 1.03             | 14.64                          | 32.06 | 2.02  | 47.82                          | 0.20 | 0.72                          | 0.05 | 98.91  |
|           | (ol)              | 36.33            | 0.02             | 0.05                           | 36.24 | 27.60 | 0.09                           | 0.35 | 0.00                          | 0.14 | 100.82 |
|           | PO4 (sp)          | 0.28             | 1.37             | 8.82                           | 32.47 | 1.52  | 54.32                          | 0.26 | 0.81                          | 0.13 | 99.98  |
|           | (ol)              | 36.20            | 0.00             | 0.02                           | 37.06 | 26.89 | 0.28                           | 0.35 | 0.00                          | 0.09 | 100.89 |
|           | PO6 (sp)          | 0.25             | 0.73             | 12.41                          | 31.86 | 1.91  | 52.18                          | 0.22 | 0.62                          | 0.02 | 100.20 |
|           | (ol)              | 35.98            | 0.02             | 0.04                           | 37.03 | 26.65 | 0.23                           | 0.37 | 0.02                          | 0.27 | 100.61 |

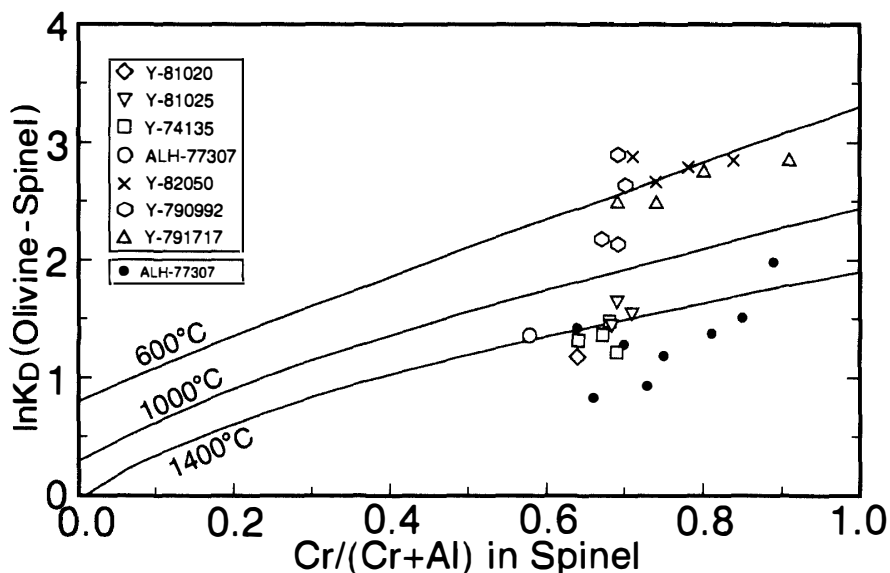


Fig. 3. Fe-Mg partitioning ( $K_D = (Fe/Mg)^{spinel} / (Fe/Mg)^{olivine}$ ) between chromites and olivine edges against Cr/(Cr+Al) ratio in chromites in type II chondrules in seven CO3 chondrites. The data of Y-81020, Y-81025, Y-74135 and ALH-77307 are plotted around 1400°C, whereas those of Y-790992, Y-791717 and Y-82050 around 600°C line. Data of ALH-77307 (filled circles) and the isotherms are quoted from JOHNSON and PRINZ (1991).

and PRINZ (1991). The data of Y-81020, Y-81025, Y-74135 and ALH-77307 are plotted around 1400°C line, whereas those of Y-790992, Y-791717 and Y-82050 around 600°C line.

### 3.2. *Cohenite and Fe-Ni metal*

Cohenite grains occur in Y-81020, Y-81025 and Y-74135, whereas no cohenite is found in Y-790992, Y-791717 and Y-82050. Table 3 shows average compositions of cohenite in Y-81025 and Y-74135. Ni contents of cohenite are generally about 4–5 wt%. It is difficult to quantify carbon contents precisely in my measurement routine. Therefore, carbon content in cohenite was analyzed qualitatively by the following method. In raw data, small CK $\alpha$  peak is detected in kamacite because of carbon coating due to conduction. In order to eliminate the contribution of coating to real CK $\alpha$  peak intensity, counts obtained from cohenite or kamacite were subtracted by counts obtained from Ni-free troilite in the same thin section. Figure 4 shows the processed peak intensity in cohenite and kamacite in Y-81020. The difference in C  $\alpha$  peak intensity between cohenite and kamacite is obvious.

Cohenite grains (<5  $\mu\text{m}$  to 200  $\mu\text{m}$  in size) occur as isolated grains or coexist with tetrataenite, troilite, kamacite and magnetite. The ordering of tetrataenite was not con-

Table 3. Average compositions (wt%) of cohenite in Y-81025 and Y-74135.

|               | Y-81025           | Y-74135           |
|---------------|-------------------|-------------------|
| No. of grains | 10                | 11                |
| Fe            | 88.02 <i>0.63</i> | 88.25 <i>0.49</i> |
| Ni            | 4.46 <i>0.25</i>  | 4.49 <i>0.17</i>  |
| Co            | 0.10 <i>0.07</i>  | 0.31 <i>0.08</i>  |
| Cr            | 0.20 <i>0.19</i>  | 0.10 <i>0.20</i>  |
| P             | 0.05 <i>0.06</i>  | 0.01 <i>0.01</i>  |
| Total         | 92.83             | 93.16             |

*Italicized figures are standard deviations of the analyses.*

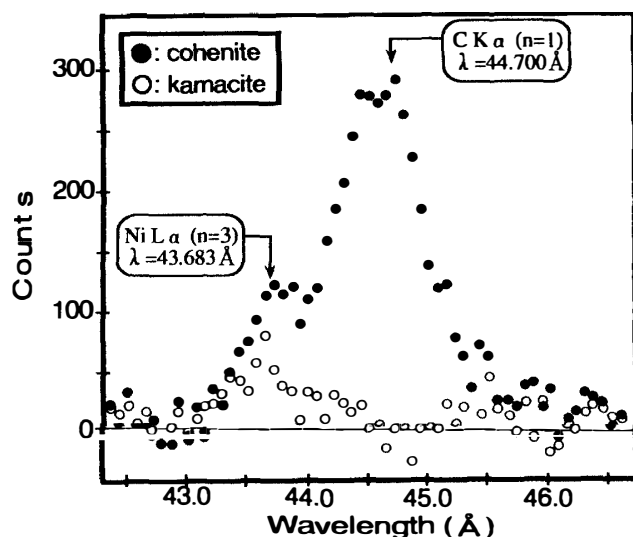


Fig. 4. Qualitative analysis of carbon in cohenite (filled circle) and kamacite (open circle) in Y-81020. These data is processed to eliminate an appearance of CK $\alpha$  peak caused by carbon coating due to conduction.

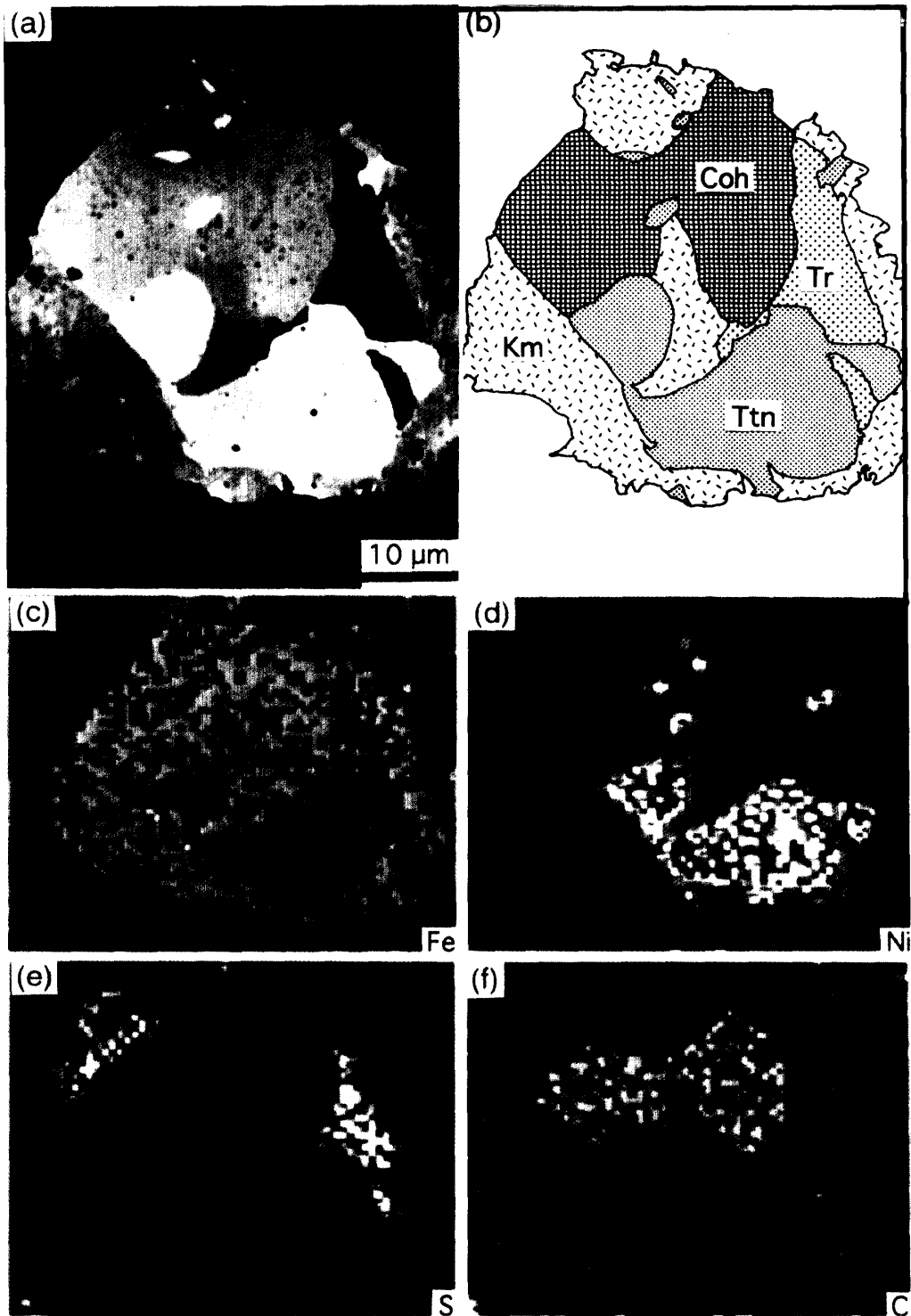


Fig. 5. The mode of occurrence of cohenite and coexisting minerals in matrix of Y-81025. (a) Back-scattered electron (BSE) image. (b) Illustration of BSE image (Coh: cohenite, Km: kamacite, Ttn: tetrataenite and Tr: troilite). (c)–(f) Elemental mappings in the same area as (a): (c) FeK $\alpha$  line, (d) NiK $\alpha$  line, (e) SK $\alpha$  line and (f) CK $\alpha$  line.

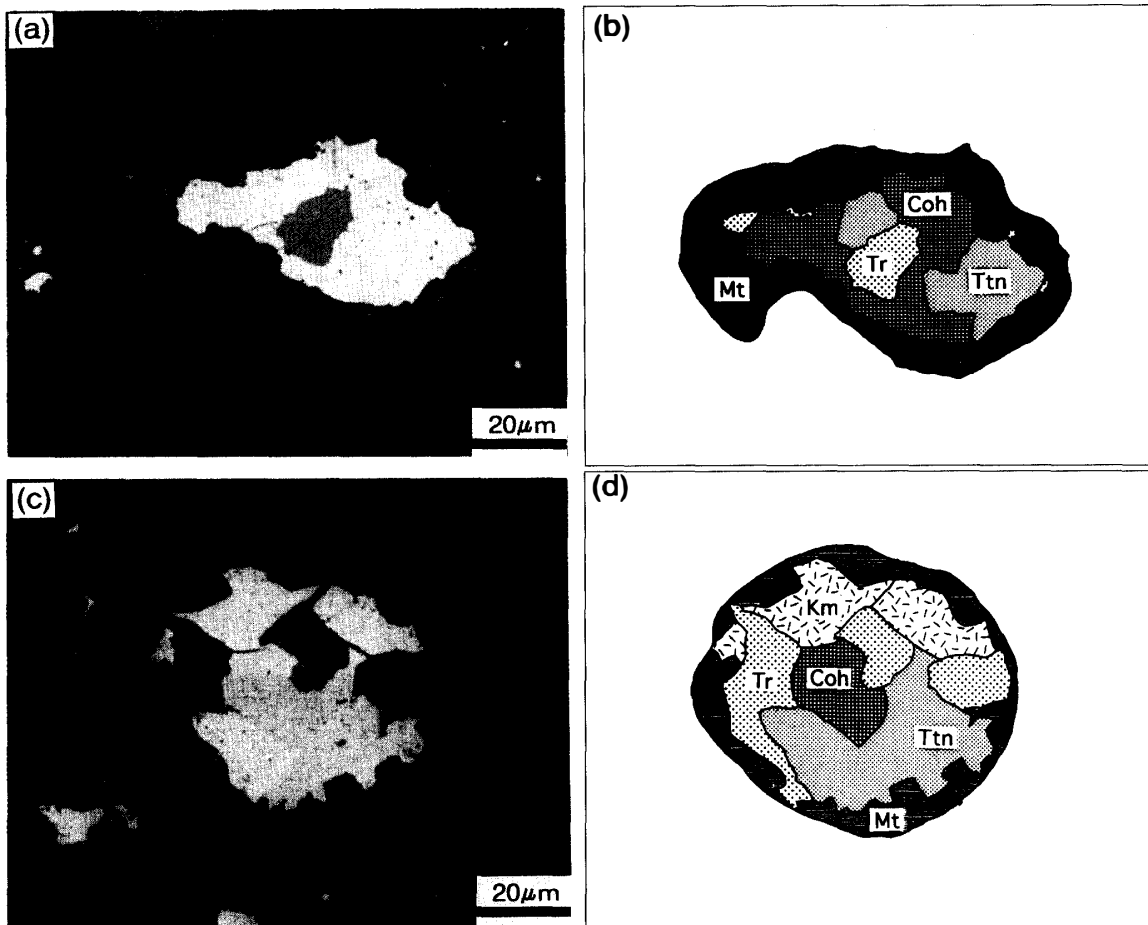


Fig. 6. The mode of occurrence of cohenite and coexisting minerals in matrix of Y-81025. (a) Photomicrograph of opaque mineral clot (reflected light). (b) Illustration of (a) (Coh: cohenite, Km: kamacite, Ttn: tetraenaite, Tr: troilite and Mt: magnetite). (c) Photomicrograph of opaque mineral clot (reflected light). (d) Illustration of (c).

firmed in this study. Here, I assume that the metal with over 49 wt% Ni is tetraenaite. Figure 5 shows a back-scattered electron (BSE) image of cohenite and coexisting minerals in Y-81025, illustration of the BSE image and elemental mapping of Fe, Ni, S and C. Figure 6 is photomicrographs and their illustrations showing the mode of occurrence of cohenite and coexisting minerals. Judging from the mode of occurrence, it seems that magnetite form by replacement process, on the contrary, it appears that cohenite does not form the intergrowth textures caused by replacement process.

Table 4 shows the percentage of Fe-Ni-C minerals (kamacite, tetraenaite and cohenite) in matrix and chondrule in Y-81025. Cohenite grains are abundant in matrix and on chondrule surface, and some occur in chondrule interior. It is clear that cohenite is not an accessory phase, but a major constituent, like as kamacite and tetraenaite.

In Y-81020, Y-81025 and Y-74135, kamacite and tetraenaite are common Fe-Ni metal phase, whereas in Y-82050, Y-790992 and Y-791717, tetraenaite is a minor phase, and kamacite and taenite are common.

Table 5 shows chemical compositions of coexisting kamacite and taenite in Y-82050,

Table 4. Percentage (vol%) of Fe-Ni-C minerals (cohenite, kamacite, tetrataenite) in matrix and chondrule in Y-81025.

|            | Cohenite | Kamacite | Tetrataenite | Numbers of grains |
|------------|----------|----------|--------------|-------------------|
| Matrix     | 65       | 20       | 15           | 78                |
| Chondrule* | 35       | 60       | 5            | 129               |

\*This means not only "in chondrule interior", but also "on chondrule surface".

Table 5. Average compositions (wt%) of Fe-Ni metal in Y-82050, Y-790992 and Y-791717.

|                 | Y-82050 |             | Y-790992 |             | Y-791717 |             |
|-----------------|---------|-------------|----------|-------------|----------|-------------|
| <b>Kamacite</b> |         |             |          |             |          |             |
| No. of grains   | 12      |             | 15       |             | 21       |             |
| Fe              | 94.43   | <i>0.78</i> | 93.90    | <i>0.74</i> | 92.82    | <i>0.73</i> |
| Ni              | 4.63    | <i>0.74</i> | 4.71     | <i>0.57</i> | 5.49     | <i>0.64</i> |
| Co              | 0.93    | <i>0.13</i> | 0.79     | <i>0.06</i> | 1.23     | <i>0.14</i> |
| Cr              | 0.11    | <i>0.17</i> | 0.11     | <i>0.17</i> | 0.05     | <i>0.07</i> |
| P               | 0.00    | <i>0.00</i> | 0.00     | <i>0.01</i> | 0.00     | <i>0.01</i> |
| Total           | 100.10  |             | 99.51    |             | 99.59    |             |
| <b>Taenite</b>  |         |             |          |             |          |             |
| No. of grains   | 12      |             | 15       |             | 21       |             |
| Fe              | 58.81   | <i>2.39</i> | 59.14    | <i>2.06</i> | 64.77    | <i>4.68</i> |
| Ni              | 40.75   | <i>2.20</i> | 39.85    | <i>1.77</i> | 33.94    | <i>4.70</i> |
| Co              | 0.17    | <i>0.03</i> | 0.14     | <i>0.02</i> | 0.40     | <i>0.12</i> |
| Cr              | 0.05    | <i>0.07</i> | 0.16     | <i>0.19</i> | 0.12     | <i>0.16</i> |
| P               | 0.00    | <i>0.01</i> | 0.00     | <i>0.01</i> | 0.00     | <i>0.01</i> |
| Total           | 99.47   |             | 99.29    |             | 99.23    |             |

Italicized figures are standards deviations of the analyses.

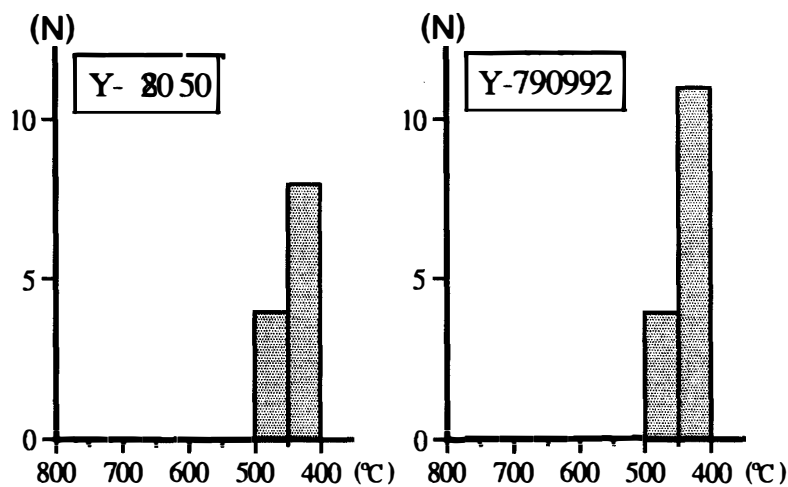


Fig. 7. Estimated temperatures based on the partition of Co between co-existing kamacite and taenite in Y-82050 and Y-790992. Estimation of temperature follows the method of AFIATTALAB and WASSON (1980).

Y-790992 and Y-791717. Analyzed points for kamacite and taenite are near the grain boundary of both phases. Figure 7 shows estimated temperatures based on the partition of Co between coexisting kamacite and taenite, using the method of AFIATTALAB and WASSON (1980). Temperatures show 400 to 500°C in Y-82050 and Y-790992. This value indicates that the metamorphic temperature of the two CO chondrites were lower than 500°C.

### 3.3. *Fine-grained opaque minerals within kamacite*

It is widely known that Fe-Ni metal often includes fine-grained silicate and phosphate minerals, however, kamacite grains in chondrule interior in Y-81020, Y-81025 and Y-74135 have fine-grained silicide and phosphide occasionally.

Figure 8a shows fine-grained perryite within kamacite in porphyritic olivine-pyroxene chondrule, which is composed of olivine ( $>Fo_{99}$ ), low-Ca pyroxene ( $>En_{98}$ ) and high-Ca pyroxene ( $En_{61}Fs_1Wo_{38}$ ), in Y-81025. Table 6 shows chemical composition of perryite. Perryite has a ideal molecular formula  $(Ni,Fe)_8(Si,P)_3$  (OKADA *et al.*, 1987). Perryite in Y-81025 is close to the ideal formula (*i.e.*,  $(Ni,Fe)_{8.3}(Si,P)_3$ ). Moreover very fine-grained Si, P-rich mineral ( $< 1 \mu m$  in diameter) in kamacite within isolated olivine occur in Y-74135. This isolated olivine resembles so-called “macroporphyritic” type I chondrule described by JONES (1992), and is composed of nearly pure forsterite ( $>Fo_{99}$ ) and a small amount of glass inclusions. Table 7 shows representative compositions of the assemblage of fine-grained Si, P-rich mineral and surrounding kamacite. Judging from the chemical composition, this Si, P-rich mineral may be very fine-grained perryite, although this fine-grained mineral is too small to analyze as individual grain. Common Fe-Ni metals in Y-81025 and Y-74135 are poor in Si, because silicate or silicide inclusion-free Fe-Ni metal grains are below 0.1 wt% Si.

Figure 8b shows very fine-grained Fe-Ni-P minerals ( $< 1 \mu m$  in diameter) within macroporphyritic type I chondrule. Table 8 shows compositions of the assemblage of fine-grained phosphide and kamacite (because this phosphide is too small to analyze as individual grain). Kamacite with fine-grained phosphide occasionally exist in other macroporphyritic type I chondrules.

Figure 8c shows fine-grained tetrataenite ( $< 1 \mu m$  to about  $5 \mu m$  in size) within kamacite in chondrule. The texture, which is composed of fine-grained tetrataenite and host kamacite, is often observed in Y-81020 and Y-81025.

### 3.4. *Magnetite*

Magnetite is abundant in Y-81020, Y-81025 and Y-74135, and coexists with Fe-Ni metal and/or troilite or occurs as isolated grain, and is richer in matrix than in chondrule interior. There are many occurrence that magnetite appears to replace Fe-Ni metal. In Y-81025, there is the characteristic texture of magnetite. Figure 9 shows assemblages of spherical magnetite (nearly pure  $Fe_3O_4$  in EPMA analysis) in matrix. These assemblages occur in voids along crack in matrix, and the texture resembles “framboidal magnetite” in CI chondrites (*e.g.*, figure in KERRIDGE *et al.*, 1979) in terms of the aggregate composed of small spherical magnetites.

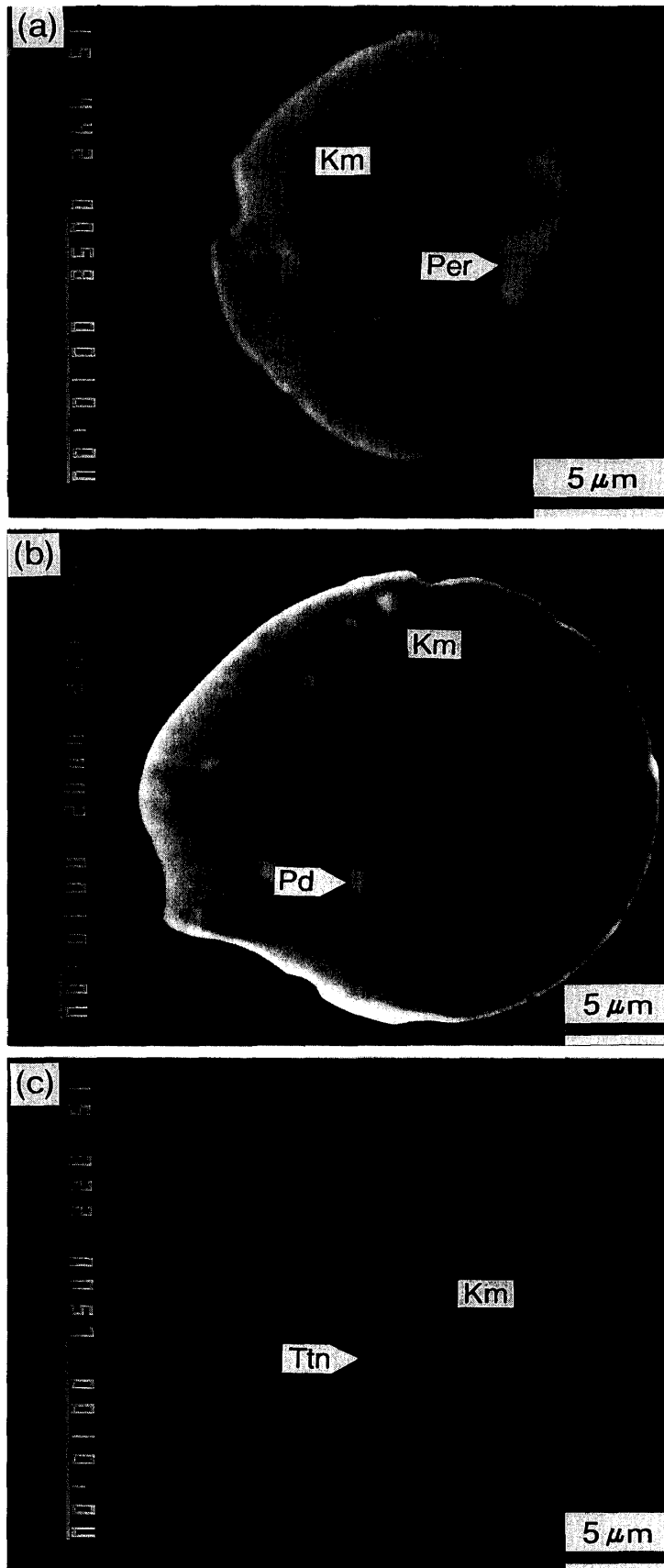


Fig. 8. BSE images of opaque minerals within kamacite (Km) in Y-81025. (a) Perryite (Per) within kamacite in macroporphyritic type I chondrule. (b) Fine-grained phosphide within kamacite. (c) Fine-grained tetraenaite (Ttn) and its host kamacite.

Table 6. Chemical compositions of perryite within kamacite in Y-81025.

| wt%   |        | atom% |       |
|-------|--------|-------|-------|
| Fe    | 8.39   | Fe    | 7.55  |
| Ni    | 76.93  | Ni    | 65.89 |
| Co    | 0.04   | Co    | 0.03  |
| Cr    | 0.06   | Cr    | 0.06  |
| P     | 5.04   | P     | 8.18  |
| Si    | 10.22  | Si    | 18.29 |
| Total | 100.68 |       |       |

Table 7. Representative compositions\* of the opaque assemblage composed of fine-grained Si, P-rich mineral and kamacite in Y-74135.

| wt%   |       |      |      |      |      |        | atom% |       |      |      |      |       |
|-------|-------|------|------|------|------|--------|-------|-------|------|------|------|-------|
| Fe    | Ni    | Co   | Cr   | P    | Si   | Total  | Fe    | Ni    | Co   | Cr   | P    | Si    |
| 28.80 | 59.86 | 0.08 | 0.39 | 2.58 | 8.90 | 100.61 | 26.52 | 52.45 | 0.07 | 0.39 | 4.28 | 16.30 |
| 97.34 | 1.52  | 0.28 | 0.24 | 0.02 | 1.29 | 100.69 | 95.52 | 1.42  | 0.26 | 0.25 | 0.04 | 2.52  |
| 87.48 | 10.35 | 0.20 | 0.10 | 0.38 | 2.24 | 100.75 | 85.13 | 9.58  | 0.18 | 0.10 | 0.67 | 4.33  |
| 64.02 | 29.89 | 0.25 | 0.06 | 1.89 | 3.61 | 99.72  | 61.95 | 27.52 | 0.23 | 0.06 | 3.30 | 6.95  |

\*Analyzed points were selected randomly in the assemblage.

Table 8. Representative compositions of the opaque assemblage composed of fine-grained phosphide and kamacite in Y-81025.

| wt%   |       |      |      |       |        |  | atom% |       |      |      |       |
|-------|-------|------|------|-------|--------|--|-------|-------|------|------|-------|
| Fe    | Ni    | Co   | Cr   | P     | Total  |  | Fe    | Ni    | Co   | Cr   | P     |
| 91.96 | 5.93  | 0.48 | 0.19 | 0.26  | 98.82  |  | 93.14 | 5.72  | 0.46 | 0.21 | 0.47  |
| 92.79 | 5.53  | 0.48 | 0.23 | 0.22  | 99.25  |  | 93.58 | 5.31  | 0.46 | 0.25 | 0.40  |
| 93.16 | 5.13  | 0.51 | 0.22 | 0.11  | 99.13  |  | 94.14 | 4.93  | 0.49 | 0.24 | 0.20  |
| 89.22 | 8.03  | 0.42 | 0.10 | 0.75  | 98.52  |  | 90.38 | 7.74  | 0.40 | 0.11 | 1.37  |
| 87.44 | 9.58  | 0.42 | 0.18 | 1.16  | 98.78  |  | 88.11 | 9.19  | 0.40 | 0.19 | 2.11  |
| 44.11 | 43.56 | 0.08 | 0.33 | 11.27 | 99.35  |  | 41.49 | 38.99 | 0.07 | 0.33 | 19.11 |
| 38.42 | 48.04 | 0.06 | 0.39 | 13.38 | 100.29 |  | 35.33 | 42.04 | 0.05 | 0.39 | 22.19 |
| 85.77 | 10.02 | 0.31 | 0.34 | 1.84  | 98.28  |  | 86.39 | 9.60  | 0.30 | 0.37 | 3.34  |
| 54.30 | 34.86 | 0.14 | 0.30 | 8.80  | 98.40  |  | 52.32 | 31.96 | 0.13 | 0.31 | 15.29 |
| 47.78 | 40.89 | 0.06 | 0.28 | 10.23 | 99.24  |  | 45.29 | 36.77 | 0.05 | 0.29 | 17.49 |

## 4. Discussion

### 4.1. Metamorphic grade of CO3 chondrites

Previous workers have studied metamorphism in the CO3 chondrite sequence (McSWEEN, 1977; SCOTT and JONES, 1990; SEARS *et al.*, 1991). Although some samples studied here already have been investigated for metamorphic grade by previous works (*e.g.*, KOJIMA *et al.*, 1995), all samples are subdivided based on petrographical investigations in this study, because subdivision of metamorphic grade is very important to dis-

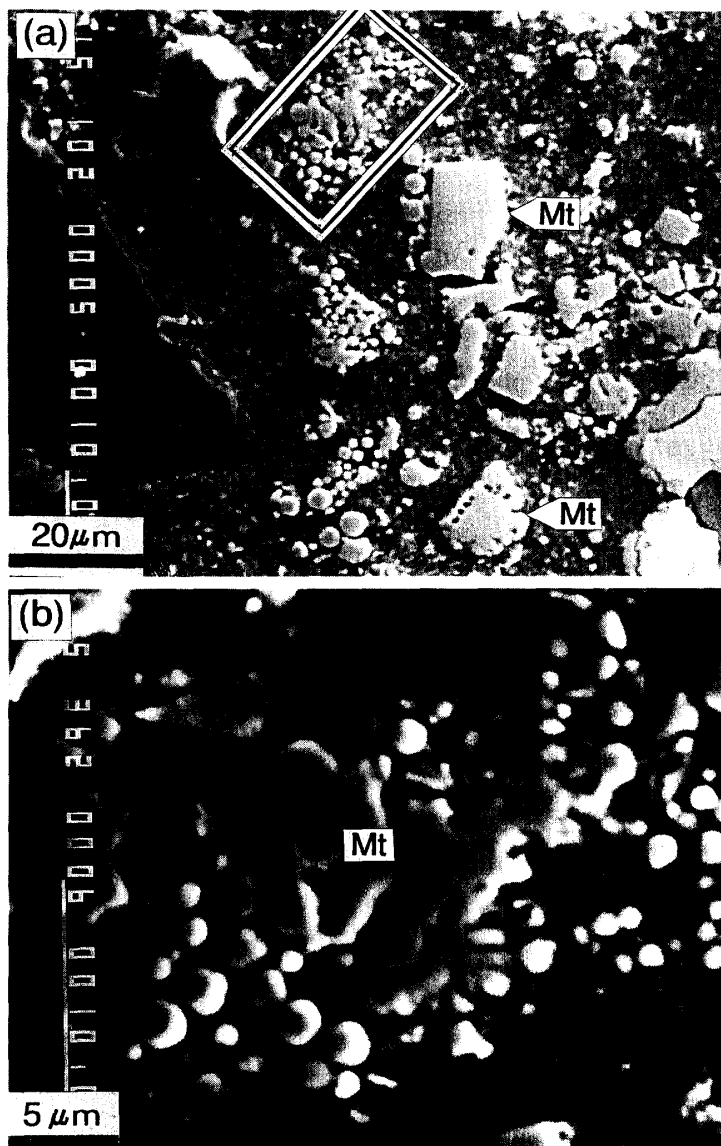


Fig. 9. Images of assemblages of spherical magnetite (Mt) in matrix of Y-81025. (a) Secondary electron image. Texture marked by arrow resemble so-called “framboidal magnetite” in CI chondrites. (b) Enlarged BSE image of boxed area in (a).

cuss about origin and evolution of opaque minerals such as Fe-Ni metal, carbides, etc.

SEARS *et al.* (1991) classified the Y-81020 as type 3.3 based on a fayalite content and TL peak at 120°C. However, they also noticed that Y-81020 display the 350°C TL peak like as the most primitive CO and CO-like chondrites (*e.g.*, ALHA77307 and Colony). KOJIMA *et al.* (1995) reported that Y-81020 as the least metamorphosed one by the further petrographical investigation. They also reported the grade of metamorphism in the three meteorites used in the study as follows; Y-81020 < Y-82050 < Y-790992. In the present study the data on the mean fayalite contents leads the following subclassifica-

tion; Y-81020, Y-81025 and Y-74135 are classified as type 3.0, Y-82050 as type 3.1, Y-790992 as type 3.2 and Y-791717 as type 3.3. The result is consistent with the metamorphic grade shown by KOJIMA *et al.* (1995).

SCOTT and JONES (1990) suggested that compositions of olivine in chondrules define clearly metamorphic grades of the host chondrites and that zoning profiles of olivine grains in type IA chondrules reflect differences in degree of metamorphic grade. Zoning profiles and compositions of olivine in type IA chondrules in Y-81025 and Y-74135 have same features, that is, low Fa mol% and increase in Cr contents from core to rim (Fig. 1). These features are consistent with data of ALHA77307 in SCOTT and JONES (1990) and that of ALH-77307 in this study. On the contrary, compositions of olivine in Y-791717 show higher Fa mol%, strong Fe zoning, low concentration of Cr and flat Cr profile (Fig. 1). These features resemble the data of Lancé, which was classified as type 3.4 in SEARS *et al.* (1991) and SCOTT and JONES (1990).

JOHNSON and PRINZ (1991) suggested that chromite-olivine pairs in type II chondrules are extremely sensitive indicators of thermal metamorphism. They pointed out that chromite-olivine pairs in chondrites of petrographic types  $\leq 3.0$  have Fe-Mg partitioning characteristic of phases which crystallized from silicate melts at the temperatures  $> 1400^{\circ}\text{C}$ , whereas pairs in chondrites of types  $> 3.0$  have partitioning characteristic of reequilibration at lower temperatures. Temperatures of pairs in Y-81020, Y-81025, Y-74135 and ALH-77307 show much higher than those of Y-790992, Y-82050 and Y-791717.

Above compositional data of olivine and chromite suggest that metamorphic grades of Y-81020, Y-81025 and Y-74135 are very low, and the same as or less than that of ALH-77307 which is widely believed in one of least metamorphosed CO3 chondrites.

#### 4.2. *Cohenite in least-metamorphic grade CO3 chondrites*

Cohenite in ALHA77307 are the first reported in carbonaceous chondrite (SCOTT and JONES, 1990). SEARS *et al.* (1991) stated that the primitive chondrite often contain carbides. In this study, I found cohenite in Y-81020, Y-81025 and Y-74135 classified as low-metamorphic grade, and no cohenite in Y-82050, Y-790992 and Y-791717 as higher metamorphic grade. Moreover, there is no report for carbides in CO3 chondrites, except in ALHA77307. Therefore, this result suggests that the existence of cohenite is indeed one of essential properties of least metamorphosed CO3 chondrite.

RUBIN *et al.* (1985) reported that no carbides were found in Colony, one of least metamorphosed CO3 chondrites. However they also reported that Colony is badly weathered, and Fe-Ni metal in matrix in Colony are replaced by mixture of limonite and  $\text{SiO}_2$  bearing material, and only Fe-Ni metal grains within olivine crystals in chondrules are observed (NOGUCHI and ISHIKAWA, 1995). The reason why cohenite does not occur in only Colony (irrespective of its low metamorphic grade) may be that cohenite have decomposed by terrestrial weathering.

As regards the formation process of cohenite, there appear to be two main possibility, namely, replacement process by diffusion of C into solid Fe-Ni metal or crystallization from Fe-Ni-C melt. Figure 10a shows kamacite, which is relatively large-size grain in Y-81025, in matrix. If C had diffused late into solid Fe-Ni metal, Fe-Ni metal surrounded by cohenite rims would have observed. However the kamacite in Fig. 10a does not coexist with cohenite, and the texture caused by replacement process is not present

at all in my thin section. Therefore, this origin can be ruled out. Although obvious evidence indicating crystallization from melt (*e.g.*, hypereutectic and/or eutectic texture as figure in GOODRICH and BERKLEY, 1986) was not found, an alternative possibility that cohenite is melt origin remains still. A petrographical evidence of severe shock metamorphism enough for generation of Fe-Ni-C melt was not found in Y-81020, Y-81025 and Y-74135. Therefore, if cohenite had formed by crystallization from Fe-Ni-C melt, timing of formation of cohenite should be during heating and the subsequent rapid cooling in stage of chondrule formation.

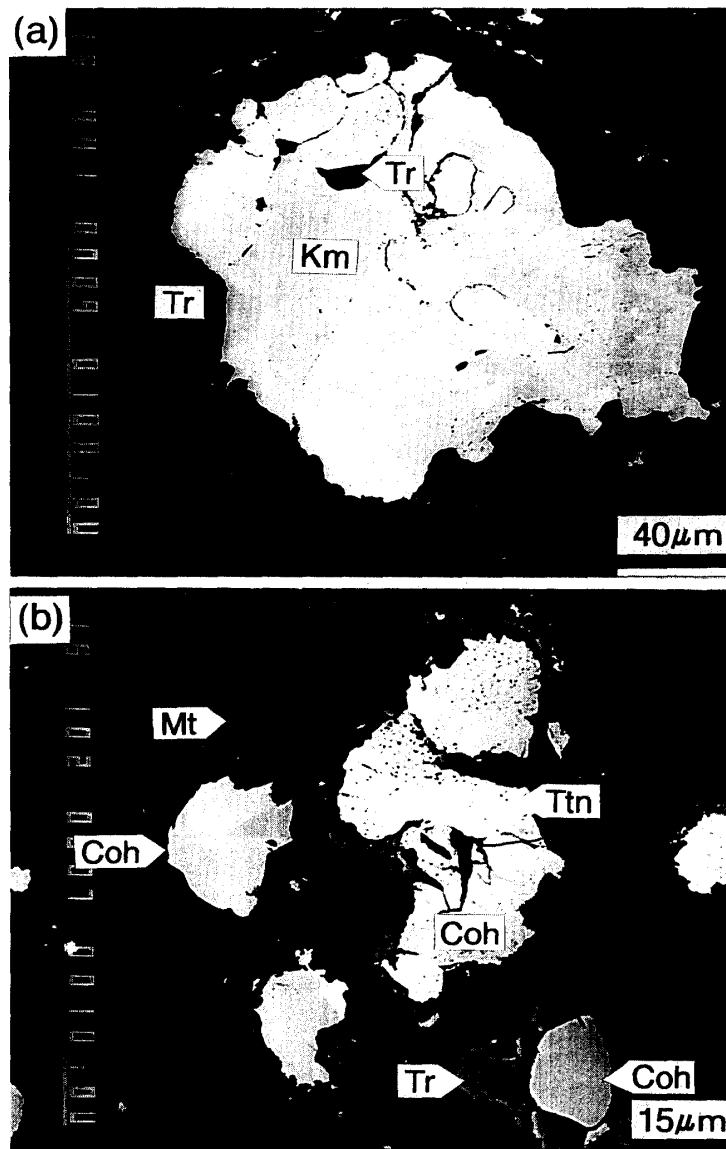


Fig. 10. BSE images of opaque minerals in matrix of Y-81025. (a) Coarse-grained kamacite (Km) coexisting with troilite (Tr). This kamacite does not coexist with cohenite. (b) Fine-grained cohenites (Coh). It appears that these cohenite remains still without break down to Fe-Ni metal and carbonaceous material.

There is a possibility for extinction of cohenite that cohenite has broken down into Fe-Ni metal and carbon due to thermal instability. According to diagram of temperature vs. time for total decomposition of cohenite (BRETT, 1967), it takes a few months at 700°C, several years at 600°C,  $10^3$  years at 500°C and  $10^6$  years (this is an extrapolated value based on BRETT's diagram) at 400°C to decompose cohenite. Metamorphic grades of Y-82050, Y-790992 and Y-791717 are higher than that of Y-81020, and estimated temperatures based on the partition of Co between coexisting kamacite and taenite in Y-82050 and Y-790992 are about 400–500°C (Fig. 7). If cohenite in these three chondrites had decomposed due to thermal instability, it could take very short times (probably a few months to several thousands years) to break down. On the contrary, even fine-grained cohenite grains (<10  $\mu\text{m}$  in size) exist in Y-81020, Y-81025 and Y-74135 (Fig. 10b). Based on olivine and chromite compositions, I can expect that the metamorphic temperatures of these chondrites are low relatively. Moreover, the occurrence of cohenite in Fig. 10b suggest definitely that the metamorphic temperatures are low (probably below 400°C) enough for the existence of fine-grained cohenite.

Besides decomposition of cohenite due to thermal instability, there are other possible explanations as to why cohenite does not occur in CO3 chondrite except least metamorphosed ones (*e.g.*, cohenite may not have formed by nature or may reduce back Fe-Ni metal and carbon by  $\text{H}_2$ ). In this study, I could not find the evidence indicating cohenite decomposed due to thermal instability (*e.g.*, intergrowths between Fe-Ni metal and carbonaceous material) in Y-82050, Y-790992 and Y-791717. Therefore, I can not specify the reason why cohenite does not exist. However, in any case, it is a proven fact that least metamorphosed CO3 chondrites such as Y-81020 are situated under low temperature condition which fine-grained cohenite remains still without breaking down.

#### 4.3. *Opaque inclusions within Fe-Ni metal and framboidal magnetite*

In Y-81020, Y-81025 and Y-74135, major Fe-Ni metals are kamacite and tetrataenite. Texture composed of fine-grained tetrataenite and host kamacite is characteristic in particularly (Fig. 8c). Tetrataenite occurs below about 450°C in Fe-Ni phase diagram (REUTER *et al.*, 1988). SMITH and LAUNSPACH (1991) pointed out that as the temperature fell through ~600°C and movement of Ni became sluggish, additional compositional changes would have been limited to those of a very local nature. The occurrence of tetrataenite in Fig. 7c would indicate that extreme sluggish Ni movement in host kamacite under low-temperature conditions (probably below 450°C) is concerned with the formation of fine-grained tetrataenite.

Moreover, texture of magnetite in Y-81025 (Fig. 9) is similar to so-called framboidal magnetite in CI chondrite. The texture in Y-81025 has formed by aqueous alteration on the parent body like that of CI chondrite, the texture also would be the evidence that Y-81025 had been situated in low-temperature environment enough for aqueous activity.

Fine-grained phosphide grains exist within kamacite in macroporphyritic type I chondrule in Y-81025. Perryite found within kamacite in porphyritic olivine-pyroxene chondrule and macroporphyritic chondrule in Y-81025 and Y-74135 is unusual mineral in carbonaceous chondrites. It is generally observed that Fe-Ni metal in chondrites often have fine-grained phosphate and silicate inclusions. In Y-81025, those inclusions are often found in Fe-Ni metal within chondrules, on the other hand, phosphide and silicide

indicating formation process under reducing condition also occur within chondrules. I do not know in detail the reason why the minerals indicating reducing condition coexist with ones indicating oxidizing condition in Y-81025. However it is a plausible explanation that formation stage of chondrules with phosphide or silicide inclusions differ from that of chondrules with oxide inclusions: for instance, genetic relationships between magnesian chondrule and ferroan chondrule in Belgica-7904 (KIMURA and IKEDA, 1992). In further study, I would like to make clear that the reason why the chondrules with inclusions indicating extremely different redox conditions coexist in same sample.

## 5. Conclusions

Based on olivine and chromite compositions, Y-81020, Y-81025 and Y-74135 are classified in least metamorphosed CO3 chondrites like as ALH-77307. The above three CO3 chondrites contain cohenites abundantly, whereas Y-82050, Y-790992 and Y-791717 which are higher metamorphic grade CO3 chondrites have no cohenite. Therefore, the existence of cohenite is indeed one of essential properties of least metamorphosed CO3 chondrites. Judging from the occurrence of cohenite, it is possible that cohenite had formed by crystallization from Fe-Ni-C melt. The existence of cohenite, fine-grained tetrataenite within kamacite, and the texture of magnetite similar to framboidal magnetite in CI chondrites suggest that above low-metamorphic grade CO3 chondrites were situated in low-temperature environment. In Y-81025 and Y-74135, there are fine-grained perryite and phosphide which are unusual minerals in carbonaceous chondrites. Origin of chondrules including perryite and the phosphide which indicate the formation process under reducing condition might differ from that of chondrules including kamacite with fine-grained phosphate and silicate.

## Acknowledgments

I am grateful to Drs. K. YANAI and H. KOJIMA of National Institute of Polar Research for giving the loan of the meteorite thin sections. I thank Prof. H. MATSUEDA of Hokkaido University for discussions and Mr. S. TERADA of Hokkaido University for help in EPMA operation.

## References

- AFIATLAB, F. and WASSON, J.T. (1980): Composition of the metal phases in ordinary chondrites: Implications regarding classification and metamorphism. *Geochim. Cosmochim. Acta*, **44**, 431–446.
- BRETT, R. (1967): Cohenite: Its occurrence and a proposed origin. *Geochim. Cosmochim. Acta*, **31**, 143–159.
- GOODRICH, C.A. and BERKLEY, J.L. (1986): Primary magmatic carbon in ureilites: Evidence from cohenite-bearing metallic spherules. *Geochim. Cosmochim. Acta*, **50**, 681–691.
- JOHNSON, C.A. and PRINZ, M. (1991): Chromite and olivine in type II chondrules in carbonaceous and ordinary chondrites: Implications for thermal histories and group differences. *Geochim. Cosmochim. Acta*, **55**, 893–904.
- JONES, R.H. (1992): On the relationship between isolated and chondrule olivine grains in the carbonaceous chondrite ALHA77307. *Geochim. Cosmochim. Acta*, **56**, 467–482.
- KERRIDGE, J.F., MACKAY, A.L. and BOYNTON, W.V. (1979): Magnetite in CI carbonaceous meteorites: Origin by aqueous activity on a planetesimal surface. *Science*, **205**, 395–397.

- KIMURA, M. and IKEDA, Y. (1992): Mineralogy and petrology of an unusual Belgica-7904 carbonaceous chondrite: Genetic relationships among the components. *Proc. NIPR Symp. Antarct. Meteorites*, **5**, 74–119.
- KOJIMA, T., YADA, S. and TOMEOKA, K. (1995): Ca-Al-rich inclusions in three antarctic CO3 chondrites, Yamato-81020, Yamato-82050 and Yamato-790992: Record of low-temperature alteration. *Proc. NIPR Symp. Antarct. Meteorites*, **8**, 79–96.
- McSWEEN, H.Y. (1977): Carbonaceous chondrites of the Ornans type: A metamorphic sequence. *Geochim. Cosmochim. Acta*, **41**, 477–491.
- NOGUCHI, T. and ISHIKAWA, K. (1995): Matrix of Colony (CO3) chondrite. *Antarctic Meteorites XX*. Tokyo, Natl Inst. Polar Res., 193–194.
- OKADA, A., ITO, T., KOBAYASHI, K. and SAKURAI, T. (1987): Crystal structure of perryite. *Papers Presented to the 12th Symposium on Antarctic Meteorites, June 8–10, 1987*. Tokyo, Natl Inst. Polar Res., 76.
- REUTER, K.B., WILLIAMS, D.B. and GOLDSTEIN, J.I. (1988): Low temperature phase transformations in the metallic phases of iron and stony-iron meteorites. *Geochim. Cosmochim. Acta*, **52**, 617–626.
- RUBIN, A.E., JAMES, J.A., KECK, B.D., WEEKS, K.S., SEARS, D.W.G. and JAROSEWICH, E. (1985): The Colony meteorite and variation in CO3 chondrite properties. *Meteoritics*, **20**, 175–196.
- SCOTT, E.R.D. and JONES, R.H. (1990): Disentangling nebular and asteroidal features of CO3 carbonaceous chondrite meteorites. *Geochim. Cosmochim. Acta*, **54**, 2485–2502.
- SCOTT, E.R.D. and TAYLOR, G.J. (1983): Chondrules and other components in C, O, and E chondrites: Similarities in their properties and origins. *Proc. Lunar Planet. Sci. Conf.*, 14th, Pt. 1, B275-B286 (*J. Geophys. Res.*, **88** Suppl.).
- SEARS, D.W.G., BATCHELOR, J.D., LU, J. and KECK, B.D. (1991): Metamorphism of CO and CO-like chondrites and comparisons with type 3 ordinary chondrites. *Proc. NIPR Symp. Antarct. Meteorites*, **4**, 319–343.
- SMITH, D.G.W. and LAUNSPACH, S. (1991): The composition of metal phases in Bruderheim (L6) and implications for the thermal histories of ordinary chondrites. *Earth Planet. Sci. Lett.*, **102**, 79–93.
- YANAI, K. and KOJIMA, H. (1987): *Photographic Catalog of the Antarctic Meteorites*. Tokyo, Natl Inst. Polar Res., 298p.
- YUI, S. (1992): A system of EPMA data reduction programs using BASIC for personal computer in 1992. *J. Fac. Sci., Hokkaido Univ.*, **23(2)**, 147–158.

*(Received July 3, 1995; Revised manuscript accepted January 5, 1996)*